

UvA-DARE (Digital Academic Repository)

The soft drop momentum sharing fraction z_g beyond leading-logarithmic accuracy

Cal, P.; Lee, K.; Ringer, F.; Waalewijn, W.J.

DOI

[10.1016/j.physletb.2022.137390](https://doi.org/10.1016/j.physletb.2022.137390)

Publication date

2022

Document Version

Final published version

Published in

Physics Letters, Section B: Nuclear, Elementary Particle and High-Energy Physics

License

CC BY

[Link to publication](#)

Citation for published version (APA):

Cal, P., Lee, K., Ringer, F., & Waalewijn, W. J. (2022). The soft drop momentum sharing fraction z_g beyond leading-logarithmic accuracy. *Physics Letters, Section B: Nuclear, Elementary Particle and High-Energy Physics*, 833, [137390].
<https://doi.org/10.1016/j.physletb.2022.137390>

General rights

It is not permitted to download or to forward/distribute the text or part of it without the consent of the author(s) and/or copyright holder(s), other than for strictly personal, individual use, unless the work is under an open content license (like Creative Commons).

Disclaimer/Complaints regulations

If you believe that digital publication of certain material infringes any of your rights or (privacy) interests, please let the Library know, stating your reasons. In case of a legitimate complaint, the Library will make the material inaccessible and/or remove it from the website. Please Ask the Library: <https://uba.uva.nl/en/contact>, or a letter to: Library of the University of Amsterdam, Secretariat, Singel 425, 1012 WP Amsterdam, The Netherlands. You will be contacted as soon as possible.

UvA-DARE is a service provided by the library of the University of Amsterdam (<https://dare.uva.nl>)



The soft drop momentum sharing fraction z_g beyond leading-logarithmic accuracy



Pedro Cal ^{a,b}, Kyle Lee ^{c,d}, Felix Ringer ^d, Wouter J. Waalewijn ^{a,b,*}

^a Institute for Theoretical Physics Amsterdam and Delta Institute for Theoretical Physics, University of Amsterdam, Science Park 904, 1098 XH Amsterdam, the Netherlands

^b Nikhef, Theory Group, Science Park 105, 1098 XG, Amsterdam, the Netherlands

^c Department of Physics, University of California, Berkeley, CA 94720, USA

^d Nuclear Science Division, Lawrence Berkeley National Laboratory, Berkeley, CA 94720, USA

ARTICLE INFO

Article history:

Received 15 August 2022

Accepted 16 August 2022

Available online 19 August 2022

Editor: B. Grinstein

ABSTRACT

Grooming techniques, such as soft drop, play a central role in reducing sensitivity of jets to e.g. underlying event and hadronization at current collider experiments. The momentum sharing fraction z_g , of the two branches in a jet that pass the soft drop condition, is one of the most important observables characterizing a collinear splitting inside the jet, and directly probes the QCD splitting functions. In this work, we present a factorization framework that enables a systematic calculation of the corresponding cross section beyond modified leading-logarithmic (MLL) accuracy, showing that this measurement is not only sensitive to the QCD charge but also the spin of the parton that initiates the jet. Our results at next-to-leading logarithmic (NLL') accuracy include non-global logarithms, and provide a first meaningful assessment of the perturbative uncertainty. We present a comparison to the available experimental data from ALICE, ATLAS, and STAR and find excellent agreement.

© 2022 The Author(s). Published by Elsevier B.V. This is an open access article under the CC BY license (<http://creativecommons.org/licenses/by/4.0/>). Funded by SCOAP³.

1. Introduction

At high-energy collider experiments, jets and their substructure play a central role in probing fundamental aspects of QCD and searching for physics beyond the standard model [1–3]. Jet grooming techniques [4–8] are designed to remove soft radiation inside jets, crucially reducing contamination in the complicated environment of hadron colliders. These techniques will become even more important during the high-luminosity era of the LHC. Grooming algorithms can also lead to significantly reduced nonperturbative (hadronization) corrections, allowing for direct and precise comparisons between theory and data, see e.g. Refs. [9–11].

In this letter, we study the soft drop grooming algorithm [8]. After reclustering a jet with the Cambridge/Aachen (C/A) [12,13] algorithm, it iteratively declusters the jet, at each step removing the softer branch if its momentum fraction z fails the soft drop condition

$$z > z_{\text{cut}} (\Delta R_{12}/R)^{\beta}. \quad (1)$$

Here, ΔR_{12} is the distance between the branches in the $y\text{-}\phi$ plane, R is the radius of the initial ungroomed jet, and z_{cut}, β are tuneable grooming parameters. (Soft drop grooming with $\beta = 0$ corresponds to the modified mass drop tagger [6].) Once Eq. (1) is satisfied, the algorithm terminates and $z_g = z$ and $R_g = \Delta R_{12}$, as illustrated in Fig. 1. Both z_g and R_g are central to characterizing the two hard branches of the groomed jet.

The momentum sharing fraction z_g has received a lot of attention by both the theoretical and experimental particle and nuclear physics communities in the past years. The main reason is that it allows for the closest to a direct measurement of the QCD (Altarelli-Parisi) splitting functions [14], providing a glimpse into fundamental splittings at parton level. The cross section differential in z_g was measured by the ALICE [15,16], ATLAS [11], CMS [17,18] collaborations at the LHC and by STAR [19] at RHIC, which we compare to in this work. In addition, the z_g distribution was also extracted from CMS open data [20,21].

This measurement is not only sensitive to the color charge but also the spin of the parton initiating the jet. Our precision is essential to have sensitivity to this effect in interpreting experimental results. The momentum sharing fraction is also of great interest for heavy-ion collisions, as it probes modifications of hard-collinear splittings in the quark-gluon plasma. For recent theoretical results, see Refs. [22–29]. We also expect z_g to be of great phenomenological importance at the future Electron-Ion Collider (EIC) [30].

* Corresponding author.

E-mail addresses: p.cal@nikhef.nl (P. Cal), kylelee@lbl.gov (K. Lee), fmringer@lbl.gov (F. Ringer), w.j.waalewijn@uva.nl (W.J. Waalewijn).

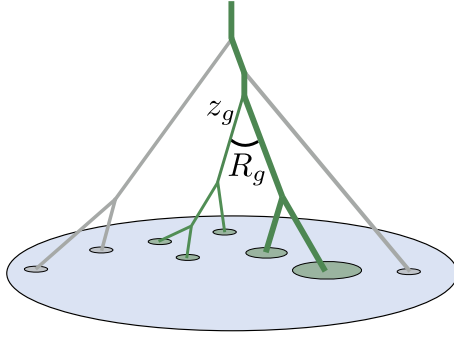


Fig. 1. Illustration of the clustering tree of a jet: Branches are groomed away (grey) until the soft drop condition in Eq. (1) is first satisfied. This splitting sets the observables z_g and R_g , and subsequent splittings (green) are kept.

The observable z_g was first introduced in Ref. [31], where a calculation of the corresponding cross section at leading-logarithmic (LL) accuracy was performed. This result was extended to modified LL (MLL) in Refs. [20,21]. It was found that z_g is Infrared-Collinear (IRC) safe only for $\beta < 0$. For $\beta \geq 0$, z_g is IRC unsafe but calculable: the IRC divergence is tamed by accounting for the Sudakov suppression, making z_g a Sudakov safe observable [32]. The cross section can thus be calculated by performing the joint resummation of the logarithms of z_g and the groomed radius R_g . Alternatively, one can impose a cut on R_g , but this case also requires resummation. Here we extend the work of Ref. [31] by setting up a factorization framework within Soft Collinear Effective Theory (SCET) [33–37], which allows for the systematic extension beyond LL. We obtain results at next-to-leading logarithmic (NLL') accuracy, accounting for non-global logarithms (NGLs) [38]. Our work also provides the first meaningful assessment of perturbative uncertainties, and opens the door to future calculations at higher perturbative accuracy and for a systematic treatment of nonperturbative effects [39,40]. Theoretical calculations of other groomed observables, such as the groomed jet mass, can be found in Refs. [41–57].

2. Theoretical framework

We now describe how we calculate the cross section differential in the jet's transverse momentum p_T and rapidity η , as well as the groomed jet substructure observables z_g and $\theta_g \equiv R_g/R$. For small jet radii, we can separate the production of the inclusive jet sample from the jet substructure measurement using collinear factorization,

$$\frac{d\sigma}{dp_T dz_g d\theta_g} = \sum_i f_i(p_T, \eta, R, \mu) \times \tilde{\mathcal{G}}_i(z_g, \theta_g, p_T R, z_{\text{cut}}, \beta, \mu). \quad (2)$$

The jet production is summarized by quark/gluon fractions $f_{i=q,g}$, which account for parton distribution functions, the hard-scattering, and semi-inclusive jet functions. The jet functions $\tilde{\mathcal{G}}_i$ (using the notation of Ref. [56]) encode the substructure measurement. See Refs. [56,58–64] for more details on this first step of the factorization.

Next, we calculate the jet function $\tilde{\mathcal{G}}_i$, which we will need to describe the region where z_g is order one. We find at leading order (LO) for $z_g, \theta_g > 0$

$$\begin{aligned} \tilde{\mathcal{G}}_q^{(1)} &= \Theta(1/2 > z_g > z_{\text{cut}} \theta_g^\beta) \Theta(\theta_g < 1) \\ &\quad \times \frac{\alpha_s}{\pi} \frac{1}{\theta_g} [P_{qq}(z_g) + P_{gq}(z_g)], \end{aligned} \quad (3)$$

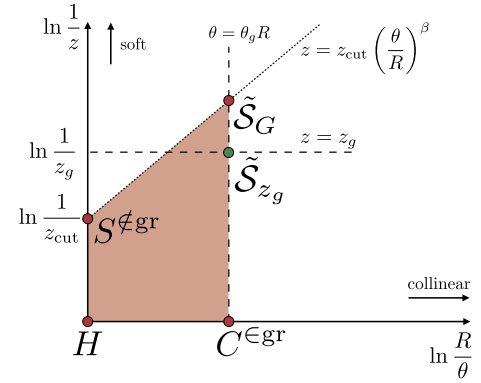


Fig. 2. Lund diagram for the cross section differential in z_g and θ_g . The green dot corresponds to the emission passing the soft drop condition, and emissions in the red area are vetoed. The modes that appear in the corresponding SCET calculation are indicated by green and red dots.

and similarly for $\tilde{\mathcal{G}}_g^{(1)}$. Here P_{ij} are the leading-order QCD splitting functions, showing that the measurement of z_g probes these. Since $\tilde{\mathcal{G}}_i^{(1)} \sim 1/\theta_g$, and there is no lower bound on θ_g for $\beta \geq 0$, we cannot integrate out the dependence on θ_g in this case. The integration over θ_g is only possible after taking into account the Sudakov suppression through resummation.

To achieve this, we perform the resummation of large logarithmic corrections of z_g, θ_g and z_{cut} . We start with the result at LL accuracy, which provides physical intuition and helps identify the relevant modes in SCET. It is described by strongly-ordered emission of gluons in the collinear and soft limit. The Lund diagram in Fig. 2 shows the phase space of such emissions in terms of their energy fraction z and angle θ , with dashed lines indicating the soft drop condition in Eq. (1) and the measurement of θ_g and z_g . The emission at the green dot sets z_g and θ_g . Emissions in the red region are not allowed, and the corresponding area enters in the Sudakov exponent:

$$\begin{aligned} \tilde{\mathcal{G}}_i &= \Theta(1/2 > z_g > z_{\text{cut}} \theta_g^\beta) \frac{2\alpha_s C_i}{\pi} \frac{1}{z_g \theta_g} \\ &\quad \times \exp \left(-\frac{\alpha_s C_i}{\pi} (\beta \ln^2 \theta_g + 2 \ln z_{\text{cut}} \ln \theta_g) \right), \end{aligned} \quad (4)$$

Here $C_{i=F,A}$ denotes the appropriate color factor for quarks and gluons, which is the only dependence on the initial parton at LL. As Eq. (4) indicates, it is now safe to integrate over θ_g due to the Sudakov suppression, and the resulting expression agrees with Eq. (14) of Ref. [31]. We note that θ_g is the natural choice as the auxiliary variable here due to the angular structure of the C/A reclustered jet. We have checked that other auxiliary observables like the jet mass are not sufficient to achieve the correct resummation even at LL.

We can extend this result to NLL' by identifying the relevant modes within SCET, for which the scaling of the momentum components can be read off from the location of the points in the Lund diagram in Fig. 2. We find

$$\begin{aligned} \tilde{\mathcal{G}}_i &= \Theta(1/2 > z_g > z_{\text{cut}} \theta_g^\beta) \tilde{H}_i(p_T R, \mu) C_i^{\text{egr}}(\theta_g p_T R, \mu) \\ &\quad \times S_i^{\neq \text{gr}}(z_{\text{cut}} p_T R, \beta, \mu) \tilde{\mathcal{S}}_G(z_{\text{cut}} \theta_g^{1+\beta} p_T R, \beta, \mu) \\ &\quad \times S_i^{\text{NG}}(z_{\text{cut}}) \left[\frac{d}{dz_g} \frac{d}{d\theta_g} \tilde{\mathcal{S}}_{z_g}(z_g \theta_g p_T R, \mu) \right. \\ &\quad \left. + \tilde{\mathcal{S}}_{i,1}^{\text{NG}}(z_g \theta_g, z_g) + \tilde{\mathcal{S}}_{i,2}^{\text{NG}}(z_g \theta_g, \frac{z_g}{z_{\text{cut}} \theta_g^\beta}) \right]. \end{aligned} \quad (5)$$

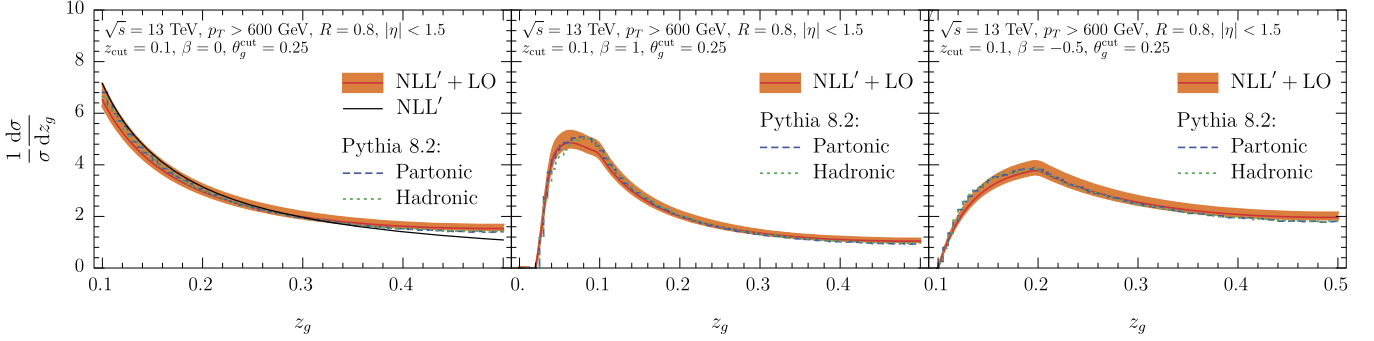


Fig. 3. Comparison of our numerical results for the momentum sharing fraction z_g at NLL'+LO to Pythia 8 simulations [65] at parton and hadron level, for representative jet kinematics and three choices of soft drop grooming parameters.

The function \tilde{S}_{z_g} is special, as it describes the single emission that sets z_g and θ_g . The collinear function C_i^{egr} describes energetic radiation at angular scales $\theta_g R$. This radiation is never groomed away, so it is constrained by the θ_g measurement. The collinear-soft radiation at the same angular scale, described by \tilde{S}_G , is furthermore subjected to the soft-drop condition in Eq. (1). Wide-angle soft radiation is always groomed away and accounted for by S_i^{egr} . Finally, the hard function \tilde{H}_i describes energetic radiation at angular scale R , and corrects for the fact that in the calculation of jet production (f_i in Eq. (2)), such radiation was unconstrained inside the jet. Except for \tilde{S}_{z_g} , these functions also appeared in the factorization of the groomed jet radius [66], and the corresponding expressions can be found there.

The resummation of logarithms of z_g , θ_g , and z_{cut} is achieved by evaluating each ingredient (except those describing NGLs) at its natural scale, which can be read off from their first argument, and using the renormalization group equations (RGEs) to evolve them to a common scale μ . We set the μ scales for the cross section differential in θ_g and cumulative in z_g , and therefore present the order α_s expression and RGE for the new ingredient \tilde{S}_{z_g} differential in θ_g :

$$\begin{aligned} \frac{d}{d\theta_g} \tilde{S}_{z_g}(z_g \theta_g p_T R, \mu) &= -\frac{2\alpha_s C_i}{\pi} \frac{1}{\theta_g} \ln \frac{\mu}{z_g \theta_g p_T R}, \\ \frac{d}{d \ln \mu} \frac{d}{d\theta_g} \tilde{S}_{z_g} &= -\frac{2\alpha_s C_i}{\pi} \frac{1}{\theta_g}. \end{aligned} \quad (6)$$

A similarly unusual RGE was encountered in Refs. [55,56], to which we refer the reader for details.

There are three types of non-global logarithms [38,67–76] in Eq. (5): First, the NGLs described by S_i^{NG} are similar to the usual hemisphere case, and arise due to correlations between the unconstrained emissions in the region outside the jet and the radiation inside the jet that fails the grooming condition. Second, the NGLs $S_{i,1,2}^{\text{NG}}$ arise from correlated emissions, where one sets z_g and θ_g (green dot) and the other is either outside the groomed radius and fails the grooming condition or inside the groomed radius and is unconstrained (corresponding to one of the two red dots on the vertical dashed line $\theta = \theta_g R$ in Fig. 2). These NGLs are sensitive to C/A clustering effects [77–79]. We include their leading contribution at order α_s^2 ,

$$\tilde{S}_{i,1}^{\text{NG},(2)}(z_g \theta_g, z_g) = 2.58 C_i C_A \left(\frac{\alpha_s}{2\pi}\right)^2 \frac{1}{z_g \theta_g} \ln z_g, \quad (7)$$

and the form of $\tilde{S}_{i,2}^{\text{NG},(2)}$ is the same at this order. In our numerical implementation these NGLs are multiplied by the global Sudakov suppression factor, see Eq. (5), making their numerical size small (percent level).

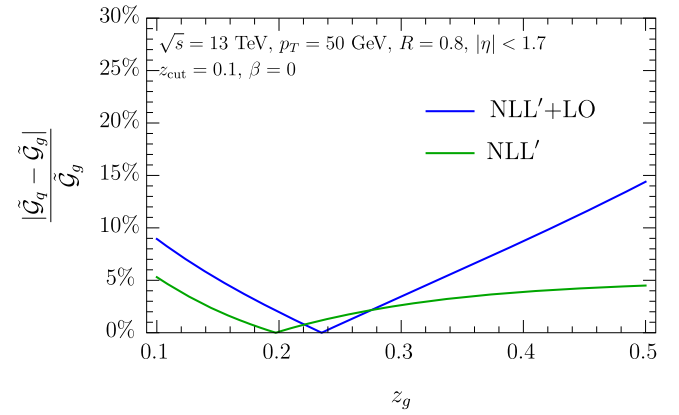


Fig. 4. Relative difference between the z_g distribution for quark and gluon-initiated jets. The difference between the green and blue curve indicates the size of the non-singular part of the QCD splitting function, encoding the spin-dependence.

3. Numerical results and comparison to data

Throughout this section we consider (ungroomed) jets which are reconstructed with the anti- k_T algorithm [80], as in the measurement of the experimental collaborations. We use the parton distribution functions of Ref. [81].

We start by comparing our numerical results at NLL'+LO accuracy to Pythia 8 simulations [65]. The comparison for exemplary jet kinematics is shown in Fig. 3. We choose three representative values of the grooming parameter β and impose a cutoff on the groomed jet radius of $\theta_g^{\text{cut}} > 0.25$ to reduce the sensitivity to nonperturbative physics. The QCD scale uncertainty bands in the figures shown here are obtained by independently varying all relevant scales in Eqs. (2) and (5) by a factor of 2 around the central scale choice. In addition, we smoothly freeze all scales at $\mathcal{O}(1 \text{ GeV})$ [82]. The hadronization corrections for the chosen kinematics are very small which can be seen by comparing Pythia results at parton and hadron level.

Overall, we observe very good agreement of our results with Pythia. In addition to the improved precision, there are notable qualitative differences with the earlier results of Ref. [31]: The shape of our distribution for $\beta < 0$ is rather different, and we find a smooth transition to $\beta = 0$ for $z_g > z_{cut}$, whether we approach from negative or positive β . This qualitative difference stems from our inclusion of additional logarithms¹ and the matching to LO given in Eq. (3). We also find that the cut imposed on θ_g gives our calculation greater perturbative stability, while qualitatively chang-

¹ We count logarithms L in the exponent. Schematically, $\ln \sigma \sim \alpha_s^n L^m$ with $m \leq n+1$.

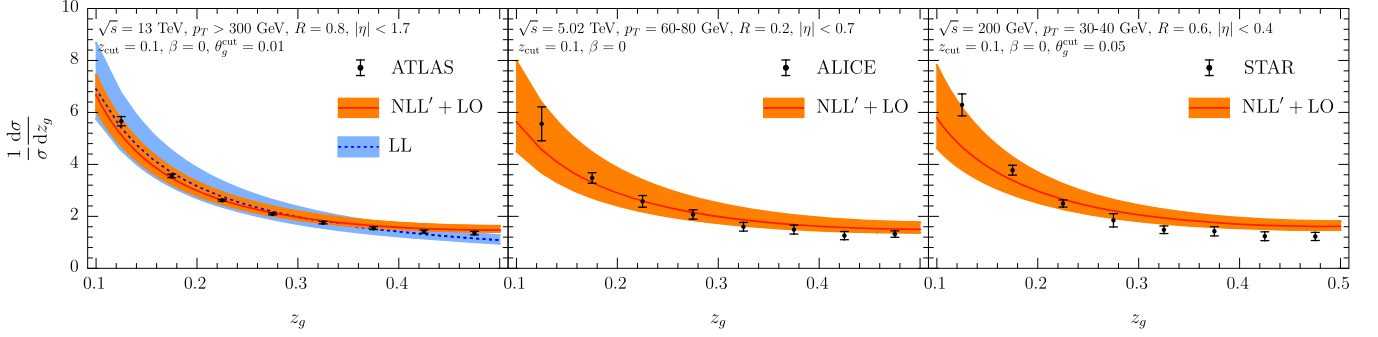


Fig. 5. Comparison of our results to ATLAS [11], ALICE [16] and STAR [19] data for $\beta = 0$.

ing the result as well. Although Ref. [31] did include the full QCD splitting function, the improved theoretical uncertainties and accuracy achieved here allow us to assess the size of the spin dependent contribution. For large z_g the matching to the LO in Eq. (3) is essential, which is done multiplicatively because of the common singularity in θ_g . Indeed, the non-singular terms added by the matching are important to achieve good agreement with Pythia, as illustrated in the left panel of Fig. 3 by the black NLL' curve (that does not include the matching). This demonstrates the sensitivity of z_g distribution to the full splitting function beyond the leading $1/z_g$ behavior in the singular limit. The size of these corrections, which encode the spin-dependence of the splitting function, are visualized in Fig. 4. Since their size can be up to order 10%, we expect that this can be probed experimentally by for example comparing inclusive vs. photon-tagged jets or jets with different rapidities.

Next, we compare to the experimental results from ATLAS [11], ALICE [16] and STAR [19] for $\beta = 0$ in Fig. 5. We normalize our results to the data² and impose the same cut on θ_g . The hadronization effects in Pythia for ALICE and STAR kinematics (not shown) are much more sizable than in Fig. 3, in accord with the larger perturbative uncertainties. Nevertheless, we find very good agreement even for these relatively low jet transverse momenta. We note that the CMS result of Ref. [17] is not unfolded, prohibiting a direct comparison. As a representative example, we show the LL QCD scale uncertainty band in the left panel of Fig. 5 which is significantly larger than at NLL'. This implies that the NLL' accuracy achieved in this work is needed to match the current experimental precision.

Next, we compare in Fig. 6 our results to ATLAS measurement [11] for $\beta = 1$, as an example. We normalize our results to the data in the region to the right of the dotted line, as our prediction for the left most data point is very sensitive to nonperturbative effects. Note that this was not needed for $\beta = 0$, where z_{cut} provides a lower bound on z_g . We observe excellent agreement! In this case our NLL'+LO prediction is substantially better than the LL result.

Lastly, we present predictions for jet kinematics at the future EIC in Fig. 7. We consider jets reconstructed in the laboratory frame $ep \rightarrow e + \text{jet} + X$ for typical EIC kinematics [83,84] with cuts on the photon virtuality Q^2 and the inelasticity y as indicated in the figure. The clean environment at the EIC will allow studies of hadronization effects, and z_g measurements in single- and di-jet events can help improve our understanding of quark/gluon differences (see also Fig. 4).

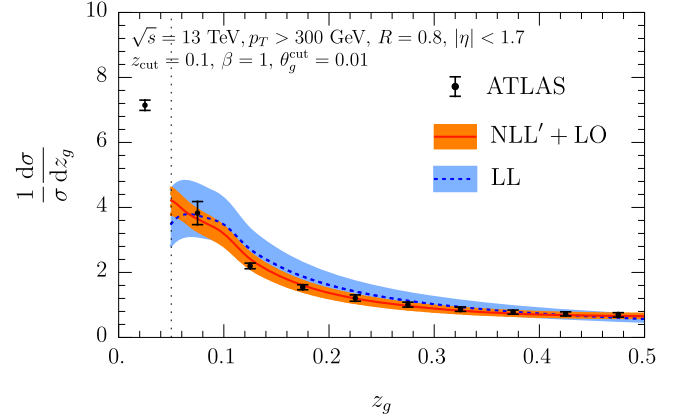


Fig. 6. Comparison to ATLAS results [11] for $\beta = 1$.

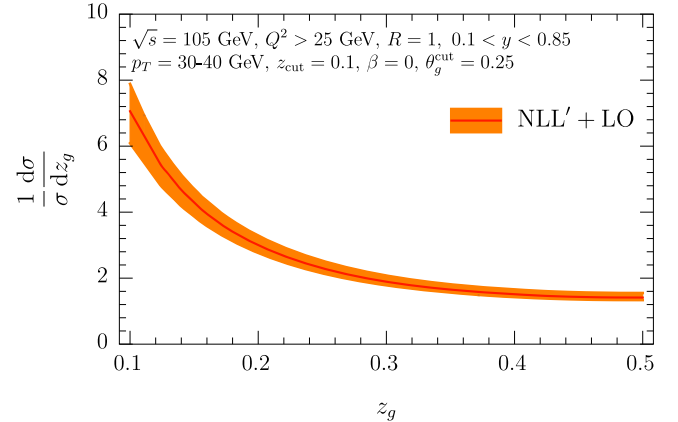


Fig. 7. Prediction for the Electron-Ion Collider.

4. Conclusions

In this work we have presented a calculation of the soft drop groomed momentum sharing fraction z_g at NLL'+LO accuracy. This Sudakov-safe jet substructure observable, which probes the hard branching process inside the jet, constitutes the closest to a direct measurement of the QCD splitting function. Our framework allows for a systematic extension beyond the previously achieved MLL accuracy, yielding qualitatively different results for $\beta < 0$ than in an earlier study, and provides the first meaningful assessment of theoretical uncertainties. Because z_g probes the full QCD splitting function, it is sensitive to the spin of the particle that initiates the jet. This effect is sufficiently large, and our calculations are sufficiently precise, to resolve it experimentally. The momentum sharing fraction z_g is one of the hallmark observables in the field

² The ALICE normalization is not normalized by a few percent, because of their treatment of jets that never pass the soft drop condition.

of jet substructure and has been measured by several experimental collaborations at the LHC and RHIC. We compared to the available experimental data and found very good agreement with our purely perturbative calculation. In addition, we provided predictions for the future Electron-Ion Collider. Our precise calculations with reliable uncertainty estimates are in excellent agreement with the data.

Declaration of competing interest

The authors declare that they have no known competing financial interests or personal relationships that could have appeared to influence the work reported in this paper.

Data availability

Data will be made available on request.

Acknowledgements

We thank Yi Chen, Raghav Elayavalli, Matt LeBlanc, Yen-Jie Lee, Ezra Lesser, James Mulligan, Ben Nachman, Mateusz Ploskon, Jennifer Roloff, and Marta Verweij for helpful discussions. We also thank Andrew Larkoski and Jesse Thaler for feedback on our manuscript. PC and WW are supported by the ERC grant ERC-STG-2015-677323, the NWO projectruimte 680-91-122 and the D-ITP consortium, a program of NWO that is funded by the Dutch Ministry of Education, Culture and Science (OCW). KL is supported by the US Department of Energy, Office of Nuclear Physics. FR is supported by the US Department of Energy under Contract No. DE-AC02-05CH11231 and the LDRD Program of LBNL.

References

- [1] A.J. Larkoski, I. Moult, B. Nachman, Jet substructure at the large hadron collider: a review of recent advances in theory and machine learning, *Phys. Rep.* **841** (2020) 1–63, arXiv:1709.04464 [hep-ph].
- [2] R. Kogler, et al., Jet substructure at the large hadron collider: experimental review, *Rev. Mod. Phys.* **91** (4) (2019) 045003, arXiv:1803.06991 [hep-ex].
- [3] S. Marzani, G. Soyez, M. Spannowsky, *Looking Inside Jets: an Introduction to Jet Substructure and Boosted-Object Phenomenology*, vol. 958, Springer, 2019, arXiv:1901.10342 [hep-ph].
- [4] D. Krohn, J. Thaler, L.-T. Wang, Jet trimming, *J. High Energy Phys.* **02** (2010) 084, arXiv:0912.1342 [hep-ph].
- [5] S.D. Ellis, C.K. Vermilion, J.R. Walsh, Recombination algorithms and jet substructure: pruning as a tool for heavy particle searches, *Phys. Rev. D* **81** (2010) 094023, arXiv:0912.0033 [hep-ph].
- [6] M. Dasgupta, A. Fregoso, S. Marzani, G.P. Salam, Towards an understanding of jet substructure, *J. High Energy Phys.* **09** (2013) 029, arXiv:1307.0007 [hep-ph].
- [7] M. Cacciari, G.P. Salam, G. Soyez, SoftKiller, a particle-level pileup removal method, *Eur. Phys. J. C* **75** (2) (2015) 59, arXiv:1407.0408 [hep-ph].
- [8] A.J. Larkoski, S. Marzani, G. Soyez, J. Thaler, Soft drop, *J. High Energy Phys.* **05** (2014) 146, arXiv:1402.2657 [hep-ph].
- [9] ATLAS Collaboration, M. Aaboud, et al., Measurement of the soft-drop jet mass in pp collisions at $\sqrt{s} = 13$ TeV with the ATLAS detector, *Phys. Rev. Lett.* **121** (9) (2018) 092001, arXiv:1711.08341 [hep-ex].
- [10] CMS Collaboration, A.M. Sirunyan, et al., Measurements of the differential jet cross section as a function of the jet mass in dijet events from proton-proton collisions at $\sqrt{s} = 13$ TeV, *J. High Energy Phys.* **11** (2018) 113, arXiv:1807.05974 [hep-ex].
- [11] ATLAS Collaboration, G. Aad, et al., Measurement of soft-drop jet observables in pp collisions with the ATLAS detector at $\sqrt{s} = 13$ TeV, *Phys. Rev. D* **101** (5) (2020) 052007, arXiv:1912.09837 [hep-ex].
- [12] Y.L. Dokshitzer, G.D. Leder, S. Moretti, B.R. Webber, Better jet clustering algorithms, *J. High Energy Phys.* **08** (1997) 001, arXiv:hep-ph/9707323 [hep-ph].
- [13] M. Wobisch, T. Wengler, Hadronization corrections to jet cross-sections in deep inelastic scattering, in: Monte Carlo Generators for HERA Physics. Proceedings, Workshop, Hamburg, Germany, 1998–1999, 1998, pp. 270–279, arXiv:hep-ph/9907280 [hep-ph], http://inspirehep.net/record/484872/files/hep-ph_9907280.pdf.
- [14] G. Altarelli, G. Parisi, Asymptotic freedom in parton language, *Nucl. Phys. B* **126** (1977) 298–318.
- [15] ALICE Collaboration, S. Acharya, et al., Exploration of jet substructure using iterative declustering in pp and Pb-Pb collisions at LHC energies, arXiv: 1905.02512 [nucl-ex].
- [16] ALICE Collaboration, J. Mulligan, Jet substructure measurements in pp and Pb-Pb collisions at $\sqrt{s_{NN}} = 5.02$ TeV with ALICE, arXiv:2009.07172 [nucl-ex], <https://alice-figure.web.cern.ch/node/16086>.
- [17] CMS Collaboration, A.M. Sirunyan, et al., Measurement of the splitting function in pp and Pb-Pb collisions at $\sqrt{s_{NN}} = 5.02$ TeV, *Phys. Rev. Lett.* **120** (14) (2018) 142302, arXiv:1708.09429 [nucl-ex].
- [18] CMS Collaboration, A.M. Sirunyan, et al., Measurement of jet substructure observables in $t\bar{t}$ events from proton-proton collisions at $\sqrt{s} = 13$ TeV, *Phys. Rev. D* **98** (9) (2018) 092014, arXiv:1808.07340 [hep-ex].
- [19] STAR Collaboration, J. Adam, et al., Measurement of groomed jet substructure observables in p+p collisions at $\sqrt{s} = 200$ GeV with STAR, *Phys. Lett. B* **811** (2020) 135846, arXiv:2003.02114 [hep-ex].
- [20] A. Larkoski, S. Marzani, J. Thaler, A. Tripathi, W. Xue, Exposing the QCD splitting function with CMS open data, *Phys. Rev. Lett.* **119** (13) (2017) 132003, arXiv:1704.05066 [hep-ph].
- [21] A. Tripathi, W. Xue, A. Larkoski, S. Marzani, J. Thaler, Jet substructure studies with CMS open data, *Phys. Rev. D* **96** (7) (2017) 074003, arXiv:1704.05842 [hep-ph].
- [22] Y. Mehtar-Tani, K. Tywoniuk, Groomed jets in heavy-ion collisions: sensitivity to medium-induced bremsstrahlung, *J. High Energy Phys.* **04** (2017) 125, arXiv: 1610.08930 [hep-ph].
- [23] Y.-T. Chien, I. Vitev, Probing the hardest branching within jets in heavy-ion collisions, *Phys. Rev. Lett.* **119** (11) (2017) 112301, arXiv:1608.07283 [hep-ph].
- [24] N.-B. Chang, S. Cao, G.-Y. Qin, Probing medium-induced jet splitting and energy loss in heavy-ion collisions, *Phys. Lett. B* **781** (2018) 423–432, arXiv:1707.03767 [hep-ph].
- [25] H.T. Li, I. Vitev, Inverting the mass hierarchy of jet quenching effects with prompt b-jet substructure, *Phys. Lett. B* **793** (2019) 259–264, arXiv:1801.00008 [hep-ph].
- [26] G. Milhano, U.A. Wiedemann, K.C. Zapp, Sensitivity of jet substructure to jet-induced medium response, *Phys. Lett. B* **779** (2018) 409–413, arXiv:1707.04142 [hep-ph].
- [27] R. Kunnnawalkam Elayavalli, K.C. Zapp, Medium response in JEWEL and its impact on jet shape observables in heavy ion collisions, *J. High Energy Phys.* **07** (2017) 141, arXiv:1707.01539 [hep-ph].
- [28] J. Casalderrey-Solana, G. Milhano, D. Pablos, K. Rajagopal, Modification of jet substructure in heavy ion collisions as a probe of the resolution length of quark-gluon plasma, *J. High Energy Phys.* **01** (2020) 044, arXiv:1907.11248 [hep-ph].
- [29] P. Cauchal, E. Iancu, G. Soyez, Deciphering the z_g distribution in ultrarelativistic heavy ion collisions, *J. High Energy Phys.* **10** (2019) 273, arXiv:1907.04866 [hep-ph].
- [30] R. Abdul Khalek, et al., Science requirements and detector concepts for the electron-ion collider: EIC yellow report, arXiv:2103.05419 [physics.ins-det].
- [31] A.J. Larkoski, S. Marzani, J. Thaler, Sudakov safety in perturbative QCD, *Phys. Rev. D* **91** (11) (2015) 111501, arXiv:1502.01719 [hep-ph].
- [32] A.J. Larkoski, J. Thaler, Unsafe but calculable: ratios of angularities in perturbative QCD, *J. High Energy Phys.* **09** (2013) 137, arXiv:1307.1699 [hep-ph].
- [33] C.W. Bauer, S. Fleming, M.E. Luke, Summing Sudakov logarithms in $B \rightarrow X_S \gamma$ in effective field theory, *Phys. Rev. D* **63** (2000) 014006, arXiv:hep-ph/0005275 [hep-ph].
- [34] C.W. Bauer, S. Fleming, D. Pirjol, I.W. Stewart, An effective field theory for collinear and soft gluons: heavy to light decays, *Phys. Rev. D* **63** (2001) 114020, arXiv:hep-ph/0011336 [hep-ph].
- [35] C.W. Bauer, D. Pirjol, I.W. Stewart, Soft collinear factorization in effective field theory, *Phys. Rev. D* **65** (2002) 054022, arXiv:hep-ph/0109045 [hep-ph].
- [36] C.W. Bauer, S. Fleming, D. Pirjol, I.Z. Rothstein, I.W. Stewart, Hard scattering factorization from effective field theory, *Phys. Rev. D* **66** (2002) 014017, arXiv: hep-ph/0202088 [hep-ph].
- [37] M. Beneke, A.P. Chapovsky, M. Diehl, T. Feldmann, Soft collinear effective theory and heavy to light currents beyond leading power, *Nucl. Phys. B* **643** (2002) 431–476, arXiv:hep-ph/0206152 [hep-ph].
- [38] M. Dasgupta, G.P. Salam, Resummation of nonglobal QCD observables, *Phys. Lett. B* **512** (2001) 323–330, arXiv:hep-ph/0104277 [hep-ph].
- [39] A.H. Hoang, S. Mantry, A. Pathak, I.W. Stewart, Nonperturbative corrections to soft drop jet mass, arXiv:1906.11843 [hep-ph].
- [40] A. Pathak, I.W. Stewart, V. Vaidya, L. Zoppo, EFT for soft drop double differential cross section, arXiv:2012.15568 [hep-ph].
- [41] C. Frye, A.J. Larkoski, M.D. Schwartz, K. Yan, Factorization for groomed jet substructure beyond the next-to-leading logarithm, *J. High Energy Phys.* **07** (2016) 064, arXiv:1603.09338 [hep-ph].
- [42] S. Marzani, L. Schunk, G. Soyez, A study of jet mass distributions with grooming, *J. High Energy Phys.* **07** (2017) 132, arXiv:1704.02210 [hep-ph].
- [43] A.J. Larkoski, I. Moult, D. Neill, Factorization and resummation for groomed multi-prong jet shapes, *J. High Energy Phys.* **02** (2018) 144, arXiv:1710.00014 [hep-ph].

- [44] Z.-B. Kang, K. Lee, X. Liu, F. Ringer, The groomed and ungroomed jet mass distribution for inclusive jet production at the LHC, *J. High Energy Phys.* **10** (2018) 137, arXiv:1803.03645 [hep-ph].
- [45] A. Kardos, G. Somogyi, Z. Trócsányi, Soft-drop event shapes in electron-positron annihilation at next-to-next-to-leading order accuracy, *Phys. Lett. B* **786** (2018) 313–318, arXiv:1807.11472 [hep-ph].
- [46] C. Lee, P. Shrivastava, V. Vaidya, Predictions for energy correlators probing substructure of groomed heavy quark jets, *J. High Energy Phys.* **09** (2019) 045, arXiv:1901.09095 [hep-ph].
- [47] Y.-T. Chien, I.W. Stewart, Collinear drop, *J. High Energy Phys.* **06** (2020) 064, arXiv:1907.11107 [hep-ph].
- [48] A.J. Larkoski, Improving the understanding of jet grooming in perturbation theory, *J. High Energy Phys.* **09** (2020) 072, arXiv:2006.14680 [hep-ph].
- [49] A. Kardos, A.J. Larkoski, Z. Trócsányi, Groomed jet mass at high precision, *Phys. Lett. B* **809** (2020) 135704, arXiv:2002.00942 [hep-ph].
- [50] D. Anderle, M. Dasgupta, B.K. El-Menoufi, J. Helliwell, M. Guzzi, Groomed jet mass as a direct probe of collinear parton dynamics, *Eur. Phys. J. C* **80** (9) (2020) 827, arXiv:2007.10355 [hep-ph].
- [51] Y. Mehtar-Tani, A. Soto-Ontoso, K. Tywoniuk, Tagging boosted hadronic objects with dynamical grooming, *Phys. Rev. D* **102** (2020) 114013, arXiv:2005.07584 [hep-ph].
- [52] J. Baron, D. Reichelt, S. Schumann, N. Schwanemann, V. Theeuwes, Soft-drop grooming for hadronic event shapes, arXiv:2012.09574 [hep-ph].
- [53] Y. Makris, Revisiting the role of grooming in DIS, arXiv:2101.02708 [hep-ph].
- [54] P. Caucal, A. Soto-Ontoso, A. Takacs, Dynamical grooming meets LHC data, arXiv:2103.06566 [hep-ph].
- [55] P. Cal, D. Neill, F. Ringer, W.J. Waalewijn, Calculating the angle between jet axes, *J. High Energy Phys.* **04** (2020) 211, arXiv:1911.06840 [hep-ph].
- [56] P. Cal, K. Lee, F. Ringer, W.J. Waalewijn, Jet energy drop, *J. High Energy Phys.* **11** (2020) 012, arXiv:2007.12187 [hep-ph].
- [57] S. Caletti, O. Fedkevych, S. Marzani, D. Reichelt, S. Schumann, G. Soyez, V. Theeuwes, Jet angularities in Z+jet production at the LHC, arXiv:2104.06920 [hep-ph].
- [58] F. Aversa, P. Chiappetta, M. Greco, J.P. Guillet, QCD corrections to parton-parton scattering processes, *Nucl. Phys. B* **327** (1989) 105.
- [59] B. Jager, A. Schafer, M. Stratmann, W. Vogelsang, Next-to-leading order QCD corrections to high p_T pion production in longitudinally polarized pp collisions, *Phys. Rev. D* **67** (2003) 054005, arXiv:hep-ph/0211007 [hep-ph].
- [60] A. Mukherjee, W. Vogelsang, Jet production in (un)polarized pp collisions: dependence on jet algorithm, *Phys. Rev. D* **86** (2012) 094009, arXiv:1209.1785 [hep-ph].
- [61] M. Dasgupta, F. Dreyer, G.P. Salam, G. Soyez, Small-radius jets to all orders in QCD, *J. High Energy Phys.* **04** (2015) 039, arXiv:1411.5182 [hep-ph].
- [62] T. Kaufmann, A. Mukherjee, W. Vogelsang, Hadron fragmentation inside jets in hadronic collisions, *Phys. Rev. D* **92** (2015) 054015, arXiv:1506.01415 [hep-ph].
- [63] Z.-B. Kang, F. Ringer, I. Vitev, The semi-inclusive jet function in SCET and small radius resummation for inclusive jet production, *J. High Energy Phys.* **10** (2016) 125, arXiv:1606.06732 [hep-ph].
- [64] L. Dai, C. Kim, A.K. Leibovich, Fragmentation of a jet with small radius, *Phys. Rev. D* **94** (11) (2016) 114023, arXiv:1606.07411 [hep-ph].
- [65] T. Sjöstrand, S. Ask, J.R. Christiansen, R. Corke, N. Desai, P. Ilten, S. Mrenna, S. Prestel, C.O. Rasmussen, P.Z. Skands, An introduction to PYTHIA 8.2, *Comput. Phys. Commun.* **191** (2015) 159–177, arXiv:1410.3012 [hep-ph].
- [66] Z.-B. Kang, K. Lee, X. Liu, D. Neill, F. Ringer, The soft drop groomed jet radius at NLL, *J. High Energy Phys.* **02** (2020) 054, arXiv:1908.01783 [hep-ph].
- [67] A. Banfi, G. Marchesini, G. Smye, Away from jet energy flow, *J. High Energy Phys.* **08** (2002) 006, arXiv:hep-ph/0206076.
- [68] A. Hornig, C. Lee, I.W. Stewart, J.R. Walsh, S. Zuberi, Non-global structure of the $O(\alpha_s^2)$ dijet soft function, *J. High Energy Phys.* **08** (2011) 054, arXiv:1105.4628 [hep-ph], Erratum: *J. High Energy Phys.* **10** (2017) 101.
- [69] R. Kelley, M.D. Schwartz, R.M. Schabinger, H.X. Zhu, The two-loop hemisphere soft function, *Phys. Rev. D* **84** (2011) 045022, arXiv:1105.3676 [hep-ph].
- [70] M.D. Schwartz, H.X. Zhu, Non-global logarithms at three loops, four loops, five loops, and beyond, *Phys. Rev. D* **90** (6) (2014) 065004, arXiv:1403.4949 [hep-ph].
- [71] S. Caron-Huot, Resummation of non-global logarithms and the BFKL equation, *J. High Energy Phys.* **03** (2018) 036, arXiv:1501.03754 [hep-ph].
- [72] Y. Hagiwara, Y. Hatta, T. Ueda, Hemisphere jet mass distribution at finite N_c , *Phys. Lett. B* **756** (2016) 254–258, arXiv:1507.07641 [hep-ph].
- [73] A.J. Larkoski, I. Moult, D. Neill, Non-global logarithms, factorization, and the soft substructure of jets, *J. High Energy Phys.* **09** (2015) 143, arXiv:1501.04596 [hep-ph].
- [74] T. Becher, M. Neubert, L. Rothen, D.Y. Shao, Effective field theory for jet processes, *Phys. Rev. Lett.* **116** (19) (2016) 192001, arXiv:1508.06645 [hep-ph].
- [75] M. Balsiger, T. Becher, D.Y. Shao, Non-global logarithms in jet and isolation cone cross sections, *J. High Energy Phys.* **08** (2018) 104, arXiv:1803.07045 [hep-ph].
- [76] A. Banfi, F.A. Dreyer, P.F. Monni, Next-to-leading non-global logarithms in QCD, arXiv:2104.06416 [hep-ph].
- [77] R. Appleby, M. Seymour, Nonglobal logarithms in interjet energy flow with k_t clustering requirement, *J. High Energy Phys.* **12** (2002) 063, arXiv:hep-ph/0211426.
- [78] Y. Delenda, R. Appleby, M. Dasgupta, A. Banfi, On QCD resummation with k_t clustering, *J. High Energy Phys.* **12** (2006) 044, arXiv:hep-ph/0610242.
- [79] D. Neill, Non-global and clustering effects for groomed multi-prong jet shapes, *J. High Energy Phys.* **02** (2019) 114, arXiv:1808.04897 [hep-ph].
- [80] M. Cacciari, G.P. Salam, G. Soyez, The anti- k_T jet clustering algorithm, *J. High Energy Phys.* **04** (2008) 063, arXiv:0802.1189 [hep-ph].
- [81] S. Dulat, T.-J. Hou, J. Gao, M. Guzzi, J. Huston, P. Nadolsky, J. Pumplin, C. Schmidt, D. Stump, C.P. Yuan, New parton distribution functions from a global analysis of quantum chromodynamics, *Phys. Rev. D* **93** (2016) 033006, arXiv:1506.07443 [hep-ph].
- [82] Z. Ligeti, I.W. Stewart, F.J. Tackmann, Treating the b quark distribution function with reliable uncertainties, *Phys. Rev. D* **78** (2008) 114014, arXiv:0807.1926 [hep-ph].
- [83] M. Arratia, Y. Song, F. Ringer, B.V. Jacak, Jets as precision probes in electron-nucleus collisions at the future electron-ion collider, *Phys. Rev. C* **101** (6) (2020) 065204, arXiv:1912.05931 [nucl-ex].
- [84] B.S. Page, X. Chu, E.C. Aschenauer, Experimental aspects of jet physics at a future EIC, *Phys. Rev. D* **101** (7) (2020) 072003, arXiv:1911.00657 [hep-ph].